Oxidative Addition of (Hetero)aryl (Pseudo)halides at Palladium(0): Origin and Significance of Divergent Mechanisms

Matthew J. Kania, Albert Reyes, and Sharon R. Neufeldt*

Department of Chemistry and Biochemistry, Montana State University, Bozeman, MT 59717, United States

Supporting Information Placeholder

ABSTRACT: Two limiting mechanisms are possible for oxidative addition of (hetero)aryl (pseudo)halides at Pd(0): a 3-centered concerted and a nucleophilic displacement mechanism. Until now, there has been little understanding about when each mechanism is relevant. Prior investigations to distinguish between these pathways were limited to a few specific combinations of substrate and ligand. Here, we computationally evaluated over 180 transition structures for oxidative addition in order to determine mechanistic trends based on substrate, ligand(s), and coordination number. Natural abundance ^{13}C kinetic isotope effects provide experimental results consistent with computational predictions. Key findings include that (1) differences in HOMO symmetries dictate that, although 12e^- PdL is strongly biased toward a 3-centered concerted mechanism, 14e^- PdL_2 often prefers a nucleophilic displacement mechanism; (2) ligand electronics and sterics, including ligand bite angle, influence the preferred mechanism of reaction at PdL_2; (3) phenyl triflate always reacts through a displacement mechanism regardless of catalyst structure due to the stability of a triflate anion and the inability of oxygen to effectively donate electron density to Pd; and (4) the high reactivity of C—X bonds adjacent to nitrogen in pyridine substrates relates to stereoelectronic stabilization of a nucleophilic displacement transition state. This work has implications for controlling rate and selectivity in catalytic couplings, and we demonstrate application of the mechanistic insight toward chemodivergent cross-couplings of bromochloroheteroarenes.

INTRODUCTION

Pd-catalyzed cross-coupling reactions of (hetero)aryl (pseudo)halides are a mainstay of organic synthesis. The catalytic cycles for these transformations begin with oxidative addition at Pd(0).[1] Because this step is often rate- and/or selectivity-determining, understanding its mechanism is valuable for improving cross-coupling methodology. Oxidative addition of aryl halides is traditionally envisioned as proceeding through a 3-centered concerted transition state.[2] However, a second limiting mechanism is also possible: the more polar "nucleophilic displacement" ("S_N"[3] or "S_NAr-like"[4]) mechanism (e.g., Scheme 1A).[5] During the nucleophilic displacement pathway, palladium does not interact significantly with the leaving group. Instead, the (pseudo)halide dissociates as an anion. At present there is minimal understanding of when each of these two mechanisms is relevant.[3,4] A recent study from our group demonstrated that the mechanism of oxidative addition can have ramifications for controlling site selectivity in cross-coupling of dichloroheteroarenes (Scheme 1B).[6] Thus, it is now clear that a better understanding of the factors controlling mechanism may facilitate rational design of selective cross-couplings.

Scheme 1. Concerted and Nucleophilic Displacement Mechanisms for Oxidative Addition at Pd(0).

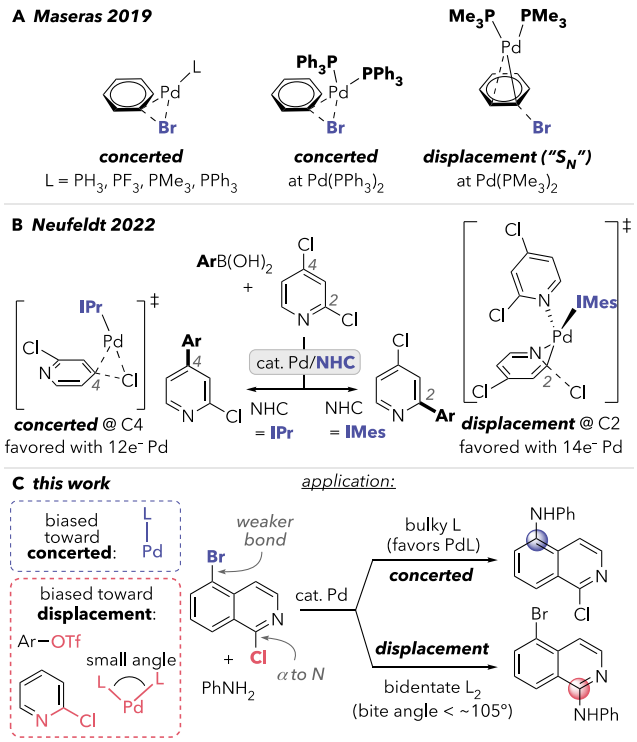

Prior reports implicate different mechanisms for a few specific combinations of substrate and ligands based on computational[3,4,6a,7–

[11] or experimental studies.[4,12–14] Maseras used density functional theory (DFT) calculations to evaluate the oxidative addition of PhBr at $12e^-$ PdL and $14e^-$ PdL_2 with a limited number of ligands (L = PH_3, PF_3, PMe_3, and PPh_3, Scheme 1A).[3] This work provided evidence that, during reaction with PhBr, PdL likely favors a concerted mechanism while the preferred mechanism for PdL_2 is ligand- and solvent-dependent.[15] Experimental Eyring parameters and Hammett values tentatively support a concerted mechanism for Ar—Br,[4] Ar—I,[12,13] and 2-pyridyl—I[4] cleavage at $Pd(PPh_3)_n$, but indicate a nucleophilic displacement mechanism for the reaction of Ph—Cl at Pd(dippp)[14] and 2-pyridyl—X (X = Cl, Br) at $Pd(PPh_3)_n$.[4] Concurrently with the present work, computations by Paci and Leitch showed that substituents on 2-chloropyridines and related compounds influence the preferred mechanism for oxidative addition at $Pd(PCy_3)_2$ due to frontier molecular orbital symmetry changes.[16]

Because prior studies comparing concerted to displacement mechanisms are limited to very few experimentally relevant ligands, we sought to computationally compare these mechanisms for a wide range of substrates and ligands. Natural abundance ^{13}C kinetic isotope effects (KIE) were also used to distinguish between mechanisms in two catalytic systems, and these experiments corroborate DFT calculations. Through molecular modeling, we find general trends that describe the mechanistic biases of PdL vs. PdL_2 as well as mechanistic preferences of different substrate classes. In a practical sense, these results emphasize that *engineering complementarity between the innate biases of the catalyst and of the substrate can enable manipulation of site selectivity in cross-coupling reactions*. We demonstrate this phenomenon in the context of cross-couplings of bromochloroheteroarenes.

COMPUTATIONAL METHODS

Calculations were performed with Gaussian 16.17 Geometry optimizations of stationary points were carried out in implicit solvent using the CPCM continuum solvation model[18] for tetrahydrofuran with the MN15L[19] functional, the LANL2DZ[20] basis set and pseudopotential for Pd and I, and a combination of 6-31+G(d) and 6-31G(d) for the other atoms (see page S20). Frequency analyses were carried out at the same level to evaluate the zero-point vibrational energy and verify the nature of the stationary points according to the appropriate number of negative eigenvalues of the Hessian matrix. The final reported energies were obtained from single point energy calculations on the optimized geometries using CPCM(THF), the MN15L functional, the SDD basis set and pseudopotential for Pd, and 6-311++G(2d,p) for all other atoms.[21,22] Gaussian 16 defaults were used for temperature and pressure (298.15 K and 1 atm). Gibbs free energy values are reported after applying Cramer and Truhlar's quasi-harmonic correction to entropy[23] with a frequency cutoff of 100 cm^{-1}. Additional computational details are available in the Supporting Information.

RESULTS AND DISCUSSION

Computational Modeling of Diverse Oxidative Addition Transition Structures. Both concerted and nucleophilic displacement transition structures were constructed for 75 combinations of PdL_n and substrate (Figure 1A). Where relevant, multiple possible ligand and substrate conformations were considered (examples in Figure 1B), and the lowest energy conformation of each type of transition structure is represented in Figure 1C. The lowest energy conformations for each mechanism type were typically those highlighted in Figure 1B (see pages S24-S29 for details on exceptions). In particular, (1) for monoligated concerted mechanisms, the ligand is usually approximately *trans* to the leaving group; (2) for monoligated displacement mechanisms, the ligand is always approximately *trans* to the *ortho* ring atom;[3] (3) for bisligated concerted mechanisms, Pd is usually pseudo-tetrahedral rather than square planar;[24] and (4) for bisligated displacement mechanisms, Pd is usually pseudo-square planar.[25] For most transition structures involving PhOTf, the sulfonyl oxygens point away from Pd. In some cases, only one mechanism type could be located. For example, some 3-centered input structures consistently optimized to nucleophilic displacement structures, and vice versa. In total, 184 unique transition structures were obtained, of which 142 represent the minimum energy geometry for a given mechanism.

We first wanted to ensure that our characterization of each output structure as "concerted" or "displacement" was reliable. Thus, three geometric parameters were analyzed for each transition structure: the Pd---C_{ipso} distance, the Pd---Y_{ortho} distance, and an adjusted value of the Pd---X distance (Figure 1C). To account for the varying atomic radii of X, the Pd---X value was normalized by measuring the difference between the Pd---X distance in the transition structure compared to a simple computed oxidative addition adduct $(PMe_3)_2Pd^{II}(Ph)X$ (X = F, Cl, Br, I, OH; see page S24). The Pd---Y_{ortho} value is defined as the distance between Pd and the nearest *ortho* ring atom (either carbon or nitrogen). These three geometric parameters for the minimum energy transition structures of each type (concerted and displacement) are plotted in Figure 1C (an animated version of this plot is available as Supplemental Information for better 3D visualization).

In the plot, the optimized structures loosely cluster into two groups representing the two limiting mechanisms. The 3-centered concerted mechanisms (circles) are characterized by shorter Pd---X distances and longer Pd---C_{ipso} and Pd---Y_{ortho} distances. Conversely, the displacement mechanisms (squares) display much longer Pd---X distances, consistent with very little interaction between Pd and the leaving group. The Pd---C_{ipso} bonds in the displacement mechanisms are essentially completely formed, with distances similar to the Pd—C bond of $(PMe_3)_2Pd^{II}(Ph)X$ (2.01 Å). Furthermore, Pd tends to lean toward one of the *ortho* atoms in the displacement mechanism as shown by the shorter Pd--- Y_{ortho} values. For PhOTf, 5-centered transition structures are also possible for oxidative addition at monoligated PdL, involving interaction between Pd and an S=O oxygen instead of the *ipso* oxygen.[10] Analysis of the three key geometric parameters revealed that the 5-centered transition structures all fall within the nucleophilic displacement cluster, not the concerted cluster. With the exception of L = IPr, the 5-centered structures are higher energy than an alternative conformation in which triflate is rotated away from Pd, so most of the 5-centered structures are not represented in Figure 1C (see Figure S8 for a version of the plot that includes these higher-energy structures).

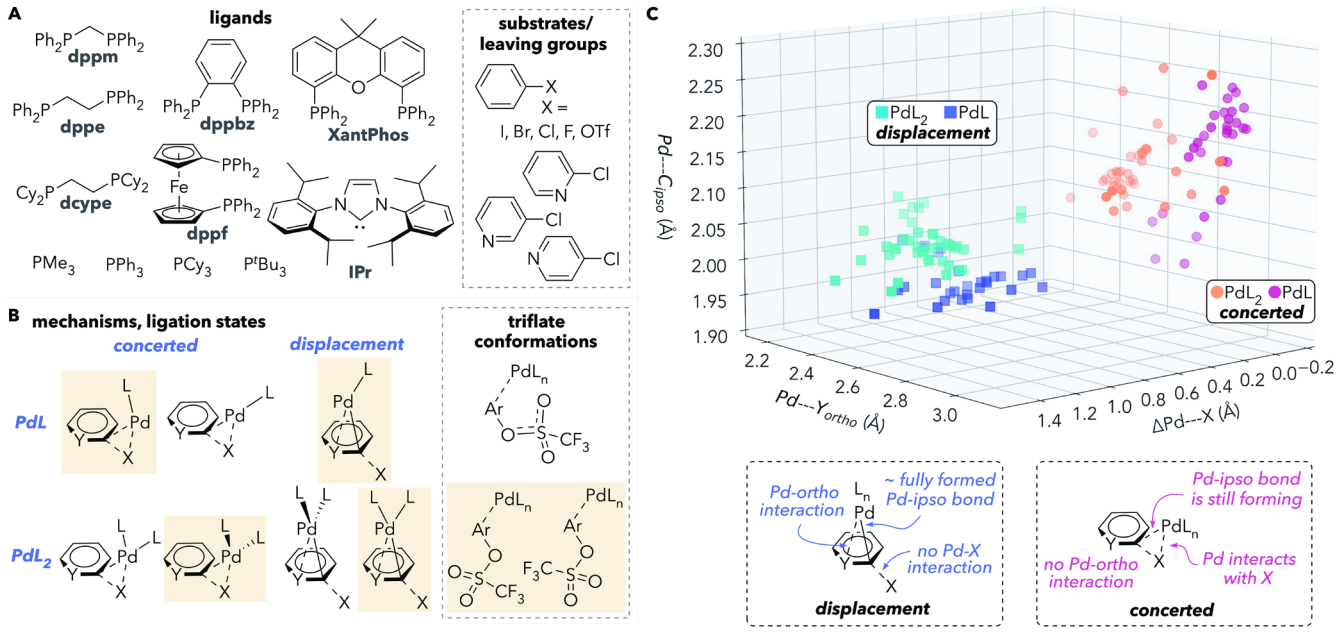

Figure 1. (A) Combinations of substrates and ligands that were computationally evaluated. (B) Mechanisms, ligation states, and conformations that were evaluated. The highlighted conformations represent those that were typically lowest energy for each mechanism type (for exceptions, see pages S24-S29). (C) Geometric parameters of the lowest-energy conformations calculated for each mechanism type.

Energetic Trends with PdL. We next compared the free energies of the concerted and displacement mechanisms for each combination of PdL_n with substrate (Figure 2). The direction of the columns in this graph indicates which mechanism is favored. In cases where only one mechanism could be located, that mechanism is assumed to be favored, although the $\Delta\Delta G^{\ddagger}$ value cannot be quantified (columns marked with an asterisk). When Pd is mono-ligated,[26] a 3-centered concerted mechanism is predicted to be favored over a displacement mechanism for all combinations of ligands with phenyl halides (Figure 2A). In several cases, only a concerted mechanism could be located. Phenyl triflate is different from the phenyl halides though: for this substrate, a displacement mechanism is favored over a concerted mechanism with all ligands. Compared to PhCl and the other chloropyridines, 2-chloropyridine shows a weaker preference for a concerted mechanism with most ligands. Together, these results indicate that monoligated Pd tends to react through a 3-centered concerted mechanism. However, aryl triflates (and, to some extent, 2-chloropyridine) are innately biased toward a displacement mechanism, and this predisposition overrides palladium's preference.

Energetic Trends with PdL_2. With bisligated PdL_2, a displacement mechanism is favored for all substrates when L = PMe_3 or L = bidentate ligands with natural bite angles smaller than ~99° (dppm, dppe, dppbz, dcype, Figure 2B).[27,28] The trend with bidentate ligands is consistent with the previously computed mechanism for oxidative addition of ArBr at Pd(dppf).[29] In several cases, only a displacement mechanism could be located. However, this trend changes with monodentate ligands PPh_3 and PCy_3, which are bulkier than PMe_3, or with the wide bite angle ligand XantPhos (natural bite angle ≈ 110°).[27,30] For these ligands, a displacement mechanism is only favored for PhOTf and 2-chloropyridine, while a concerted mechanism is favored for phenyl halides. These results suggest that PdL_2 is innately predisposed to react through a displacement mechanism, although a large L—Pd—L bite angle can mitigate this bias. A triflate leaving group or an α-nitrogen predisposes the substrate for a displacement mechanism: this mechanism is favored for PhOTf and 2-chloropyridine, even with Xantphos and all of the monodentate ligands.

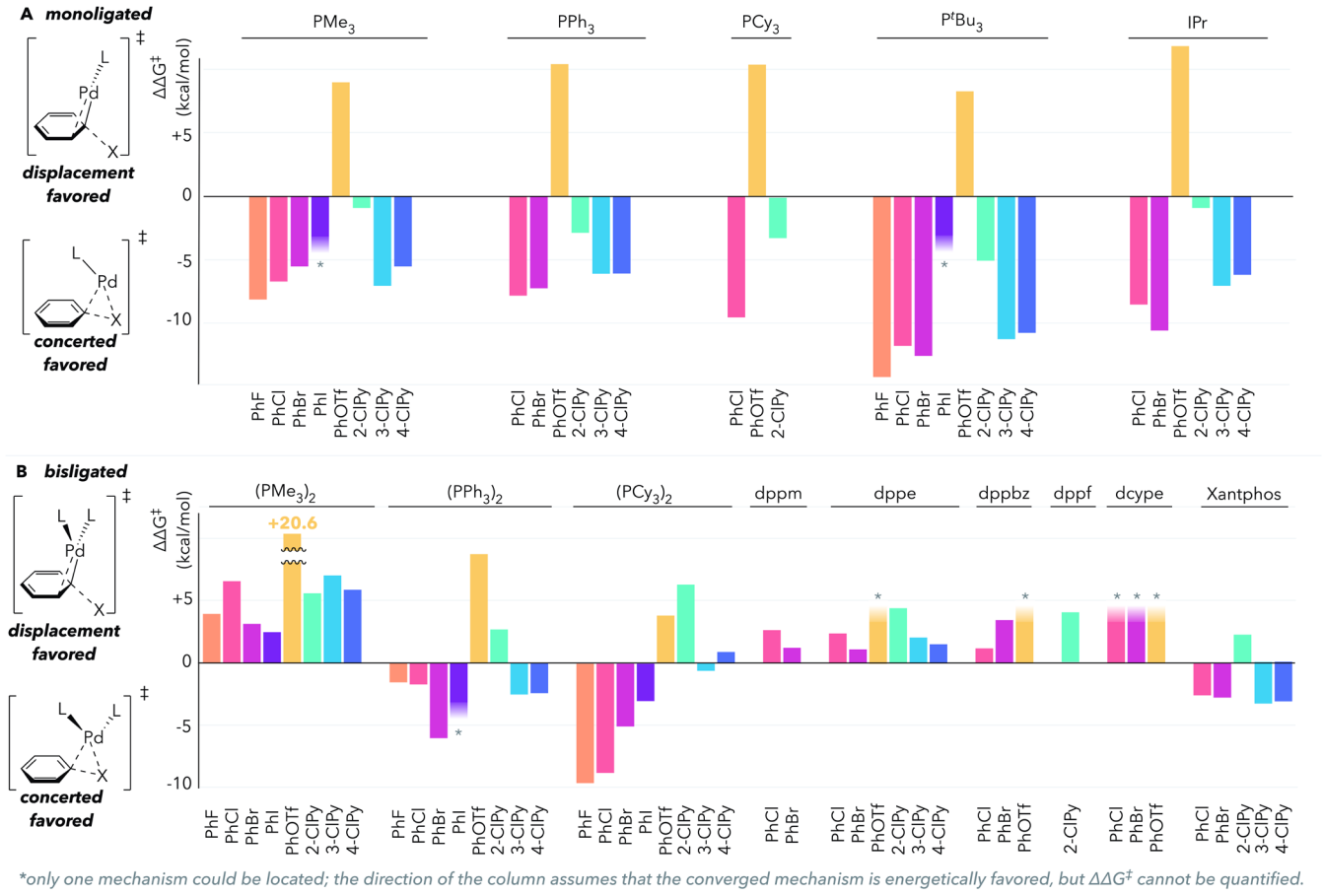

*only one mechanism could be located; the direction of the column assumes that the converged mechanism is energetically favored, but ΔΔG‡ cannot be quantified.

Figure 2. Difference in free energies of activation for displacement versus concerted transition structures for (A) monoligated Pd and (B) bisligated Pd.

Overview of ^{13}C KIE Studies. DFT calculations give predictions that can be sensitive to method choice.[31] Thus, we next sought to check our calculations against experimental results. Our calculations predict the relative free energies of two types of transition structures (3-centered concerted vs. displacement) for each combination of ligand, substrate, and coordination number. Relative free energies of activation ($\Delta\Delta G^{\ddagger}$ values) are often measured experimentally by comparing product ratios. However, product ratio measurements are not applicable to distinguishing mechanisms of oxidative addition for these substrates, since both transition structures would ultimately lead to the same products in catalytic reactions (and likely also in stoichiometric reactions).[32] Thus, we turned to natural abundance ^{13}C KIE quantitative NMR studies using the method developed by Singleton.[33,34] We anticipated that the two mechanisms could be distinguished by ^{13}C KIE values at the *ipso* position of the substrate due to differences in the vibrational modes involving that carbon during the corresponding transition structures.

We selected two Pd-catalyzed Suzuki cross-coupling systems to study: (1) reaction of the aryl chloride **1** using the bulky monodentate ligand P^{t}Bu$_3$ and (2) reaction of aryl triflate **2** using PPh$_3$ (Scheme 2). Both reactions were conducted in THF. The *tert*-butyl group on the substrates serves as an internal isotope standard, with the KIE at the methyl carbons assumed to be 1.000. Each cross-coupling reaction was run on a 16.0 mmol scale to ~80-92% conversion. The unreacted substrate was recovered and its carbon isotope distribution was compared to the isotope distribution in a standard sample (a sample of substrate from the same source that had not been subjected to the cross-coupling conditions). The changes in integrations at each position relative to the 1° carbons of *tert*-butyl were used to calculate ^{13}C KIE values (see pages S4–S14 for details). These experimental KIE values were then compared to the values predicted by DFT.[35] The experimental KIE values reflect the isotopic sensitivity of the first substrate-committing step, which is expected to be C—X cleavage in all cases. Formation of a π-complex between Pd and substrate precedes C—X cleavage in these systems, but calculations at the level of theory used herein suggest that this step is reversible and has a much lower barrier than C—X cleavage, so it should not contribute significantly to the observed KIE values (see pages S35-S36).[36] All DFT KIE values represent the average of several dispersion-containing DFT methods (see pages S37-S44). Experimental KIE values are reported as an average representing 6 FIDs for each of 2 separate trials (the KIE from each trial is reported separately). For each KIE value, the number in parentheses represents the error in the final digit based on a 95% confidence interval (see pages S4–S14).

Scheme 2. ^{13}C Kinetic Isotope Effect Studies Indicate (A) a Concerted Mechanism for Oxidative Addition of a Chloroarene at Pd(P^tBu_3) and (B) a Displacement Mechanism for Oxidative Addition of an Aryl Triflate at $Pd(PPh_3)_2$.

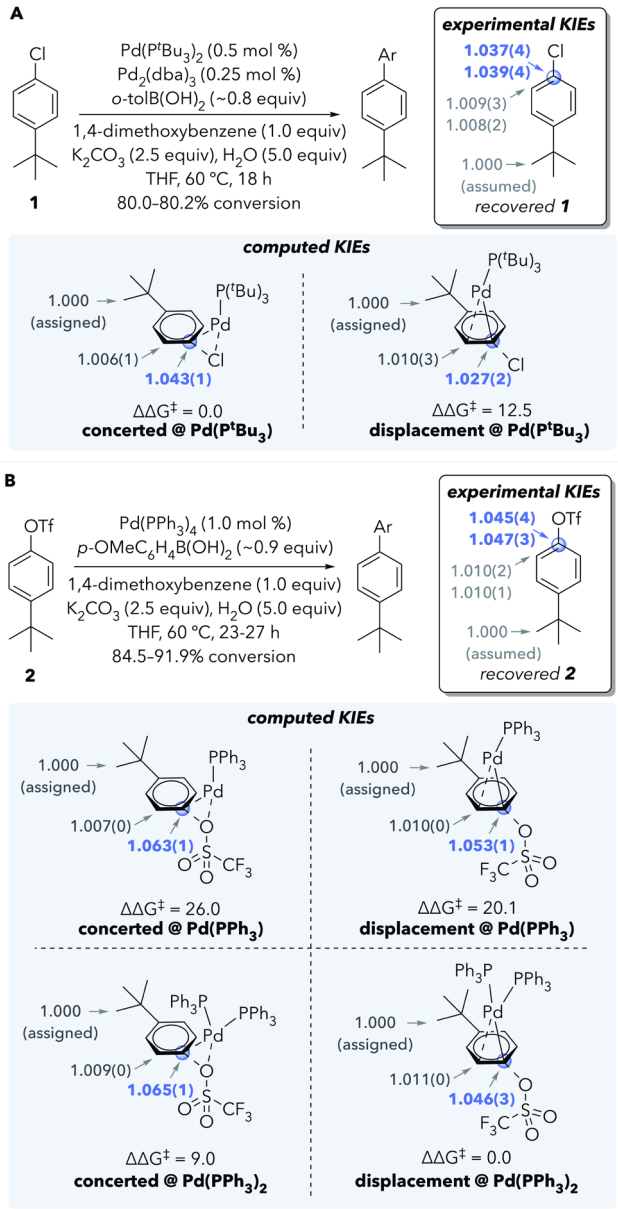

Experimental KIE values reported for two separate trials. The number in parentheses represents the error in the final digit based on a 95% confidence interval. Computed ΔΔG‡ values in kcal/mol are reported relative to the lowest energy transition structure for each reaction, averaged across at least 9 DFT methods (see SI)

^{13}C KIE Studies on an ArCl/P^{t}Bu$_3$ System. Our DFT calculations indicate that monoligated Pd(P^{t}Bu$_3$) strongly prefers to react with aryl chlorides through a 3-centered concerted mechanism over a nucleophilic displacement mechanism [$\Delta\Delta G^‡$ = 12.5 kcal/mol for **1** (Scheme 2) and $\Delta\Delta G^‡$ = 11.8 kcal/mol for PhCl, Figure 2A]. Reaction at Pd(P^{t}Bu$_3$)$_2$ is not possible with such a bulky ligand.[37,38] There is evidence that oxidative addition may be possible at bisligated Pd(P^{t}Bu$_3$)(solv) in coordinating solvents like MeCN or DMF, but not in THF.[22] Accordingly, just two mechanisms were considered with this ligand (Scheme 2): a 3-centered concerted mechanism and a nucleophilic displacement mechanism at monoligated Pd(P^{t}Bu$_3$). The computed KIE at C_{ipso} is larger for the concerted mechanism [1.043(1)] than the displacement mechanism [1.027(2)], which is consistent with prior observations comparing concerted versus step-wise mechanisms for S_N2 and S_NAr reactions.[39] The computed 2° KIE values at C_{ortho} are much smaller than at C_{ipso}, but slightly larger for the displacement mechanism—in which Pd interacts with the *ortho* atom—compared to the concerted mechanism. For the Suzuki coupling of **1** catalyzed by Pd/P^{t}Bu$_3$, we obtained experimental KIE values at C_{ipso} of 1.037(4) and 1.039(4), which are similar to the computed KIE for the 3-centered concerted mechanism, and significantly larger than the computed KIE for the displacement mechanism. The experimental KIE value at C_{ortho} is not useful for distinguishing mechanisms as it is within error of both computed values. Overall, the experimental KIE values at C_{ipso} support the computational prediction that a 3-centered concerted mechanism at monoligated Pd(P^{t}Bu$_3$) is favored for oxidative addition of aryl chlorides.

^{13}C KIE Studies on an ArOTf/PPh$_3$ System. Our calculations indicate that the lowest energy pathway for oxidative addition of aryl triflates is a nucleophilic displacement mechanism involving PdL_2 when L = PPh$_3$ (Scheme 2). Prior literature suggests that PPh$_3$ may promote reaction at either PdL or PdL_2.[4,38,40] For example, Hirschi and Vetticatt proposed that aryl bromides react at monoligated Pd(PPh$_3$) under Suzuki-Miyaura catalytic conditions using $Pd(PPh_3)_4$.[40] The computed transition structure for this oxidative addition is best described as a 3-centered concerted mechanism. On the other hand, Maes and Jutand demonstrated that 2-chloropyridines react with bisligated $Pd(PPh_3)_2$ through a displacement (S_NAr-like) mechanism.[4] Thus, four mechanisms were computationally considered for oxidative addition of aryl triflates at Pd/PPh$_3$: (1) 3-centered at Pd(PPh$_3$) [computed KIE of 1.063(1) at C_{ipso}]; (2) displacement at Pd(PPh$_3$) [computed KIE of 1.053(1)]; (3) 3-centered at $Pd(PPh_3)_2$ [computed KIE of 1.065(1)]; and (4) displacement at $Pd(PPh_3)_2$ [computed KIE of 1.046(3)]. For the Suzuki coupling of **2** catalyzed by Pd/PPh$_3$, we obtained experimental KIE values at C_{ipso} of 1.045(4) and 1.047(3), which most closely match the computed KIE for displacement at $Pd(PPh_3)_2$. As such, the experimental KIE is consistent with the computational prediction that a nucleophilic displacement mechanism at bisligated $Pd(PPh_3)_2$ is favored for oxidative addition of aryl triflates. This outcome is also consistent with other literature evidence suggesting that aryl triflates react preferentially at PdL_2.[37a,37c,38,41] Furthermore, in combination with Hirschi and Vetticatt's report, this result demonstrates that the mechanism of oxidative addition at Pd/PPh$_3$—both its geometry as well as palladium's coordination number—may change when comparing aryl bromides to triflates. Finally, the near agreement between the computationally predicted and experimentally implicated mechanisms for both the ArCl/P^{t}Bu$_3$ (*vide supra*) and the ArOTf/PPh$_3$ systems suggests that meaningful conclusions can be drawn from the DFT data.

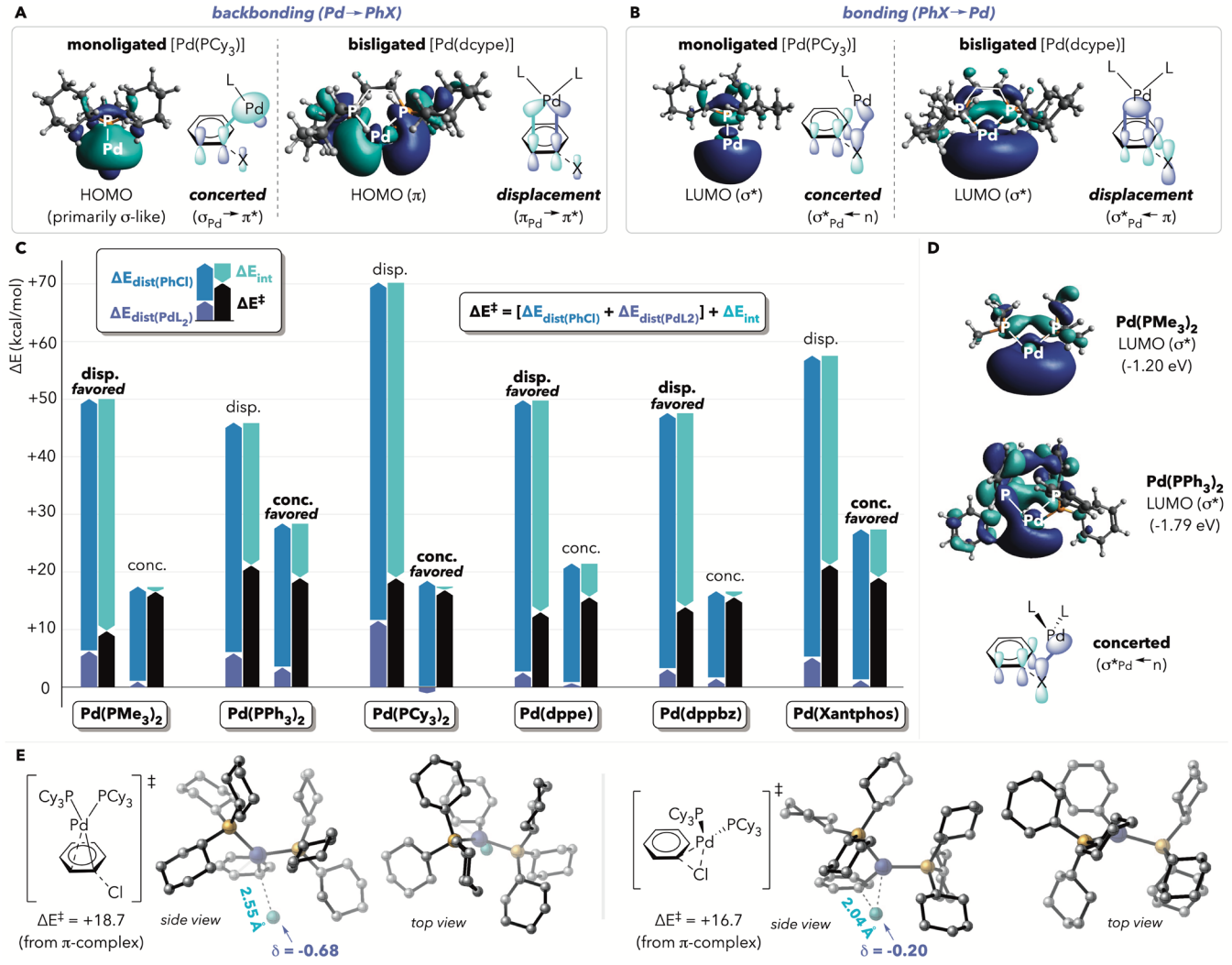

Figure 3. (A) The HOMO symmetry of PdL predisposes it to donate into a single ring atom, while the HOMO symmetry of PdL_2 is best suited to donate into two ring atoms. (B) The LUMOs of PdL and PdL_2 both have σ-symmetry. (C) Distortion-interaction analysis of oxidative addition of PhCl at PdL_2. All energies are measured relative to the preceding PhCl-PdL_2 π-complex. (D) The lower energy LUMO of $Pd(PPh_3)_2$ compared to $Pd(PMe_3)_2$ facilitates stronger interaction during a concerted mechanism via donation from chloride non-bonding electrons. (E) Bisligated displacement transition structures experience more distortion energy for both the catalyst and substrate fragments because of more crowding between fragments and a more product-like Ph—Cl distance. Calculated NBO charges on chloride are shown. On 3D images, hydrogens are hidden for clarity.

Why Do PdL and PdL_2 Have Different Mechanistic Preferences? For reactions with phenyl halides, PdL always reacts through a 3-centered mechanism, whereas PdL_2 often prefers a displacement mechanism. These differences can be understood on the basis of frontier molecular orbitals.[6a,11,42] Mono- and bisligated Pd use filled orbitals of different symmetry to donate electron density into an aryl (pseudo)halide π* orbital (Figure 3A). The HOMO of PdL resembles an L—Pd σ/d_z^2 hybrid, and it interacts with the substrate in a primarily σ fashion (Figure 3A, left). Thus, PdL can effectively donate electron density to only a single atom of the substrate (C_{ipso}). In contrast, when PdL_2 is bent into a geometry appropriate for interacting with the substrate, the HOMO is d_{xy}-like and presents π-symmetry with two equally sized lobes of opposite phases. Therefore, the HOMO of PdL_2 can achieve good orbital overlap with the substrate's π* orbital by interacting with a second atom that has an antibonding relationship to C_{ipso} (Figure 3A, right).[43] For all of the substrates we investigated, even in the ground state there is a larger π* orbital coefficient at an *ortho* ring atom compared to the (pseudo)halide leaving group (e.g., 13% at C_{ortho} vs. 9% at Cl for undistorted PhCl; see Figure 4B), which is consistent with PdL_2 preferring to interact with C_{ortho}. The LUMOs of both PdL and PdL_2 have σ-symmetry (Figure 3B), so the shape of these unoccupied orbitals is less relevant to determining the preferred mechanism.

How Do Ancillary Ligand Sterics and Bite Angle Affect Mechanism for PdL_2? As observed by Maseras,[3] our calculations suggest that 14e^- PdL_2 may react through either a concerted or displacement mechanism, depending on its ligands. To better understand the effect of ligands on the mechanistic preference of PdL_2, we conducted a distortion-interaction analysis on several of the transition structures involving PhCl (Figure 3C).[44] For this analysis, each transition structure was separated into two distorted fragments, PdL_2 and PhCl. Distortion energies for each fragment [$\Delta E_{dist(PdL2)}$ and $\Delta E_{dist(PhCl)}$] were calculated by comparing the distorted fragments to the corresponding fragments derived from the preceding π-complex.

The interaction energy between the fragments (ΔE_{int}) is calculated as the difference between the energy of the transition state ($\Delta E^{\ddagger}$) and the sum of the distortion energies (ΔE_{dist}). Total distortion energies are positive (unfavorable), while interaction energies are typically negative (favorable).

In general, both the catalyst and the PhCl fragments experience much more distortion in displacement transition structures compared to concerted ones. The geometry of the transition structures is consistent with this trend: in a displacement mechanism, the catalyst fragment has more overlap with the plane of the arene (leading to crowding between the phosphine ligands) and the C—Cl distance is more product-like compared to a concerted mechanism (Figure 3E). Thus, for a sufficiently bulky ligand like PCy_3, the preference for a concerted mechanism is distortion-controlled: there is a particularly large amount of distortion experienced by both $Pd(PCy_3)_2$ and PhCl in a displacement mechanism, while the catalyst fragment actually experiences a slight relief of distortion in the concerted mechanism (compared to the preceding π-complex).[45,46] On the other hand, displacement transition structures benefit from much larger interaction energies. The large interaction energy during displacement mechanisms is consistent with stronger overlap between the catalyst's HOMO and chlorobenzene's π* orbital (*vide supra*). Therefore, when sterics are not a significant factor (for PMe_3 and the small bite angle diphosphines dppe and dppbz),[47] the preference for a displacement mechanism is primarily interaction-controlled.

A comparison between PPh_3 and PMe_3/PCy_3 suggests that ligand electronics also play a role in the favored mechanism. PPh_3 is not a particularly bulky ligand, but $Pd(PPh_3)_2$ still prefers a concerted mechanism for reaction with PhCl. Both the distortion and the interaction energies in a displacement mechanism with $Pd(PPh_3)_2$ are small compared to mechanisms involving $Pd(PMe_3)_2$ and $Pd(PCy_3)_2$. However, the interaction energy during a concerted mechanism with $Pd(PPh_3)_2$ is relatively large (Figure 3C), which may be attributed to Cl → σ^*_{Pd} bonding (Figure 3D). Donation from halide to Pd is expected to be stronger when Pd has a lower energy LUMO (is more electron-deficient), as in the case of Pd supported by triarylphosphines. Similarly, the displacement mechanism involving $Pd(PPh_3)_2$ does not benefit from as much interaction energy as a mechanism involving trialkylphosphines because the HOMO of $Pd(PPh_3)_2$ is lower-energy (see page S45) and it cannot donate as strongly into the PhCl π* orbital.

Why are Aryl Triflates Biased Toward a Displacement Mechanism? Our calculations indicate that PhOTf uniformly prefers to react through a nucleophilic displacement mechanism, even with monoligated PdL (see Figure 2 and Scheme 2B). This prediction is consistent with experimental studies demonstrating that (a) oxidative addition of triflates leads to cationic complexes,[48] (b) oxidative addition of triflates at PdL_2 is faster in more polar media,[49] and (c) aryl triflates are extremely unreactive toward monoligated PdL[22,37,49,50] (PdL is biased toward a concerted mechanism). This extremely strong preference of triflates to react through a displacement mechanism can be understood in part based on triflate's stability as an anion. Displacement transition structures are much more polar than concerted structures, with a high degree of negative charge buildup on the leaving group (examples in Figure 3E).[4,7,8,14] Triflate is better able to accommodate this charge compared to any of the halides,[11] as evidenced by the acidity of its conjugate acid [pKa of TfOH in DCE = –11.3, compared to HBr (–4.4) and HCl (0.2)].[51] Conversely, the high energy of concerted transition structures involving triflate can be understood based on frontier molecular orbital interactions. During oxidative addition, orbital mixing between the catalyst and substrate fragment occurs in both directions (to a first approximation, $HOMO_{Pd}$ → $\pi^*_{substrate}$ as well as $\pi/n_{substrate}$ → $LUMO_{Pd}$). Analysis of the PhX molecular orbitals indicates that interaction between Pd and triflate in a concerted mechanism is disfavored because triflate bears a particularly small coefficient in both the HOMO and π* orbitals (Figure 4). For example, only 7% of the HOMO of PhOTf resides on the C—O oxygen atom, compared to a much larger contribution from the halides of PhCl or PhBr (25% and 30%, respectively, Figure 4A). The relatively small coefficient on oxygen is consistent with the more intuitive concepts of hard and soft, where oxygen is a harder, more electronegative atom with lower-energy valence electrons. Thus, in a 3-centered concerted mechanism, Pd receives relatively little stabilization of its building positive charge when interacting with oxygen compared to one of the halides. The *ortho* carbon of PhOTf has a larger HOMO coefficient (15%) than oxygen, so orbital mixing with palladium's LUMO is more effective during a displacement mechanism. For orbital mixing in the other direction ($HOMO_{Pd}$ → $\pi^*_{substrate}$), PhOTf is again biased against a concerted mechanism because the oxygen of the C—O bond has a very small π* coefficient compared to the halides in the analogous PhX substrates (3%, 9%, and 10% on O, Cl, and Br, respectively, Figure 4B).

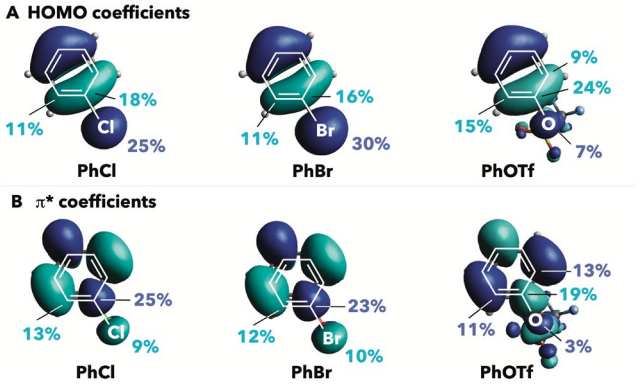

Figure 4. (A) Percent contributions of halide (or oxygen), C_{ipso}, and C_{ortho} to the highest occupied molecular orbital of PhX substrates. (B) Percent contribution of the same atoms to the lowest energy unoccupied molecular orbitals that do not contain a node passing through C—X (LUMO+1 for PhCl and PhBr, and LUMO for PhOTf).

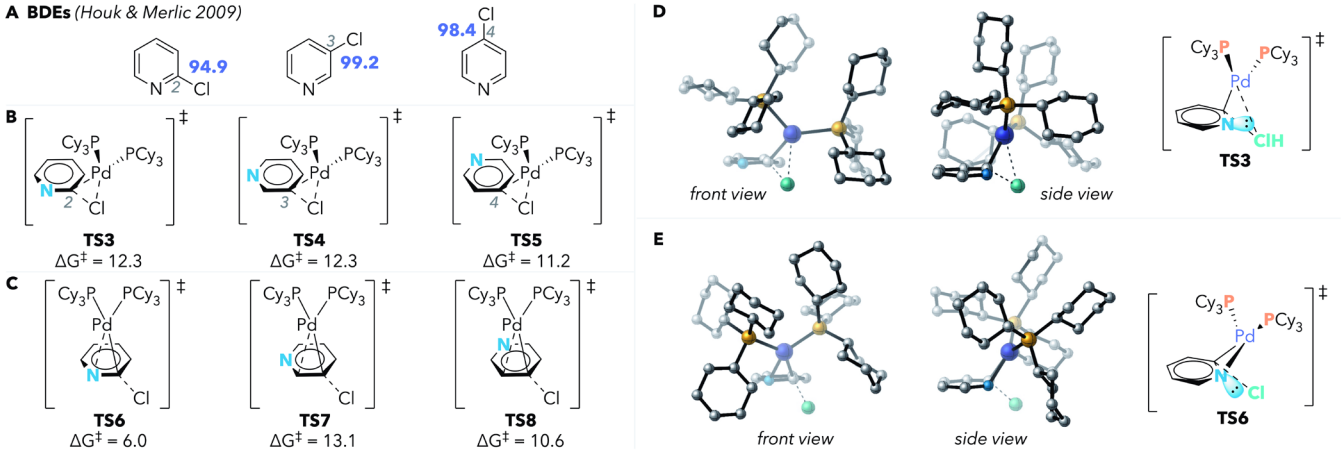

Figure 5. (A) Bond strengths do not trend with (B) the energies of concerted mechanisms for oxidative addition at $Pd(PCy_3)_2$, but they do trend with (C) the energies of displacement mechanisms at $Pd(PCy_3)_2$. (D) A concerted mechanism for reaction of 2-chloropyridine does not benefit from stereoelectronic C—Cl weakening in the same way as (E) a displacement mechanism. Free energies of activation in (B) and (C) are measured relative to separated reactions chloropyridine + $Pd(PCy_3)_2$.

Why Does an Adjacent Nitrogen Atom Bias the Mechanism Toward Displacement? Nitrogen atoms in 6-membered heteroarenes have long been considered to have an activating effect on adjacent C—X bonds. For example, 2,x-dihalopyridines (x = 3, 4, or 5) usually undergo cross-coupling selectively at the C2—halide.[52] Houk and Merlic noted that a trend in bond strengths could explain this preference: the C—X bond α to nitrogen is weaker than a more distal C—X bond (Figure 5A).[53] Nevertheless, monoligated PdL and some Pd clusters have recently been shown to react at the more distal, stronger C4—X bond of 2,4-dihalopyridines,[6,54,55] suggesting that an adjacent nitrogen primarily activates C—X bonds toward reaction with $14e^-$ PdL_2 (not $12e^-$ PdL). Our calculations show that PdL_2 strongly prefers to react with 2-chloropyridine through a displacement mechanism, even when supported by ligands that promote a concerted reaction for aryl halides (PPh_3, PCy_3, Xantphos, see Figure 2B).[11] We hypothesized that the conventionally high reactivity of C—X bonds adjacent to nitrogen is intimately tied to their preference for a displacement mechanism.

Supporting this hypothesis, we found that *concerted* activation barriers for oxidative addition of 2-, 3-, and 4-chloropyridine at $Pd(PCy_3)_2$ are nearly identical and do not trend with bond dissociation energies (Figure 5B). That is, even though C2—Cl is a weaker bond in the ground state, it is not necessarily easier to break through a concerted mechanism. This result indicates that, at least with $Pd(PCy_3)_2$, the lower C2—Cl bond dissociation energy is primarily advantageous during a displacement mechanism. A C2—Cl bond is remarkably easy to break through a displacement mechanism (Figure 5C). Analysis of transition state geometries suggests that stereoelectronic factors play a role in favoring a displacement mechanism for C2—Cl. In the ground state of 2-chloropyridine, the C—Cl bond is weakened because of the neighboring lone pair.[53b,56] Nitrogen's lone pair resides in an orbital that is parallel to C2—Cl, and thus destabilizes this bond through hyperconjugation.[56,57] During oxidative addition through either mechanism, the C—Cl bond is distorted out of the plane of the pyridine ring. In a concerted mechanism, distortion of the C—Cl bond means that it is no longer parallel to the non-bonding orbital on nitrogen, so some of nitrogen's bond-weakening effect is lost (Figure 5D). Conversely, in a displacement mechanism in which nitrogen forms a partial bond to Pd, the nitrogen atom adopts a pseudo-tetrahedral electronic geometry (Figure 5E).[58] Thus, the orbital containing nitrogen's lone pair remains largely parallel to the C—Cl bond even as it distorts out-of-plane, and the lone pair continues to facilitate C—Cl cleavage through hyperconjugation. In addition to this stereoelectronic effect, we also considered whether a proximal nitrogen enables more favorable charge distribution than a distal nitrogen during displacement transition states. However, NBO charge calculations suggest that charge distributions do not play a significant role in the relative energies of **TS6**-**TS8** (see pages S45-S46).

Practical Implications: Dihaloheteroarene Site Selectivity. This work highlights that the preferred mechanism for oxidative addition is influenced by both ligand and substrate. Thus, engineering complementarity between catalyst and substrate should enable control of site selectivity through control of the oxidative addition mechanism. To test this hypothesis, we evaluated three 2-chloropyridine derivatives that also contain a bromide distal to nitrogen. Aryl bromides are usually considered to be more reactive than chlorides in cross-coupling reactions due to the relative weakness of a C—Br bond. However, in these substrates, a displacement mechanism for oxidative addition of the C—Cl bond would be especially stabilized by an interaction between Pd and the *ortho* nitrogen. Accordingly, the use of bidentate ligands that promote a nucleophilic displacement mechanism would complement the substrate bias for reaction at the C2—Cl bond through a displacement mechanism. Conversely, the use of ligands that favor a concerted mechanism would mitigate the stabilizing influence of the *ortho* nitrogen, and preferential reaction at the weaker C—Br bond is expected.

Consistent with this hypothesis, substrates **9**-**11** preferentially undergo catalytic amination at bromide when using bulky monodentate ligands P^tBu_3 or SIPr (Scheme 3). These ligands should promote reaction at PdL,[38,50c] which generally prefers a concerted mechanism. On the other hand, bidentate ligands with moderate bite angles[59] promote reaction at the chloride next to nitrogen.[60] In these cases, reaction at PdL_2 through a displacement mechanism is

expected. In contrast, more reaction at the distal bromide is observed with the wide bite-angle ligand Xantphos. Notably, the chemoselectivity trends with **9** are consistent with observations reported by Ji[61] and by Tan and Sigman[62] for catalytic amination.

Scheme 3. Ligands that Promote a Displacement Mechanism Favor Reaction at C—Cl Adjacent to N, While Ligands that Promote a Concerted Mechanism Favor Reaction at a Distal C—Br.[a]

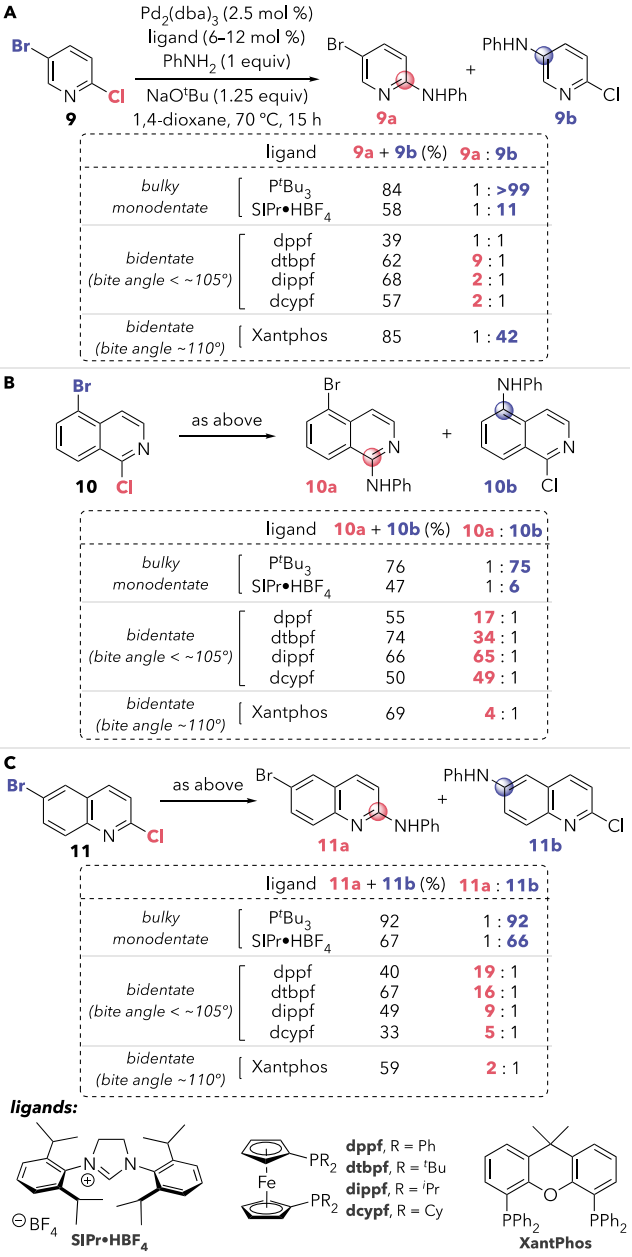

[a]Monodentate ligands were loaded at 12 mol %, bidentate ligands at 6 mol %. GC-FID yields calibrated against undecane as an internal standard, average of 2 trials.

CONCLUSION

The broad computational study presented herein illustrates clear trends in the preferred mechanism for oxidative addition at Pd^0 based on substrate, ligand(s), and palladium's coordination number. ^{13}C KIE studies on a system involving a 3-centered concerted mechanism and one involving a nucleophilic displacement mechanism provide experimental support for the DFT calculations. The predicted mechanistic biases suggests a strategy for chemodivergent cross-coupling of bromo-2-chloropyridine derivatives, and this work demonstrates the realization of that strategy through rational ligand variation.

Because oxidative addition is often the rate- or selectivity-determining step of cross-couplings, the ability to predict its mechanism can facilitate finding the right match between substrate and catalyst to achieve faster reactions or higher site-selectivity. The key findings in this work can be summarized through a set of suggested guidelines for predicting the likely mechanism of oxidative addition of aryl electrophiles at Pd(0):

(a) With aryl halides, a 3-centered concerted mechanism is likely when using traditional monodentate phosphines (including PPh_3). Depending on the size of the monodentate ancillary ligand and the identity of the halide, oxidative addition may take place at PdL, which uniformly prefers a concerted mechanism. Alternatively, oxidative addition may take place at PdL_2, which is also likely to favor a concerted mechanism unless L is very small (e.g., PMe_3), due in part to steric crowding in the displacement mechanism.

(b) On the other hand, aryl halides are more likely to react through a displacement mechanism when employing bidentate phosphines with conventional bite angles (< ~105°) due in part to the strong interaction energy between catalyst and substrate fragments in a displacement mechanism and minimization of unfavorable distortion energy.

(c) Aryl triflates essentially always react through a displacement mechanism. This preference can be attributed to the stability of anionic triflate and the weak coordinating ability of triflate oxygens to Pd.

(d) For halides adjacent to pyridine nitrogens, the displacement mechanism is particularly favored in part because of a stereoelectronic effect by which a nitrogen lone pair weakens the C—X bond during a displacement mechanism.

These guidelines can serve as a starting point[63] for rationally engineering cross-coupling outcomes when oxidative addition is the selectivity-determining or turnover-limiting step.

AUTHOR INFORMATION

Corresponding Author

* Email: sharon.neufeldt@montana.edu.

ORCID

Matthew J. Kania: 0000-0003-4445-9780; Albert Reyes: 0000-0001-8944-6444; Sharon R. Neufeldt: 0000-0001-7995-3995.

Notes

The authors declare no competing financial interest.

ASSOCIATED CONTENT

Supporting Information

The Supporting Information is available free of charge on the ACS Publications website.

Experimental and computational details, NMR spectra, and calculated energies (PDF)

Cartesian coordinates of minimum-energy calculated struc-tures (XYZ)

Animated version of Figure 1C (MP4)

NMR spectra for KIE studies (ZIP)

ACKNOWLEDGMENT

This work was supported by NSF (CHE-1848090 and CHE- 2400070). The computational studies used Expanse at the San Diego Supercomputer Center and Bridges-2 at the Pittsburgh Supercomputing Center through allocations CHE-170089 and CHE-230031 from the Advanced Cyberinfrastructure Coordination Ecosystem: Services & Support (ACCESS) program, which is supported by NSF grants #2138259, #2138286, #2138307, #2137603, and #2138296. Computational efforts were also performed on the Tempest High Performance Computing System, operated and supported by University Information Technology Research Cyberinfrastructure at Montana State University. Support for MSU's NMR Center was provided by the NSF (Grants NSF-MRI:CHE-2018388 and NSF-MRI:DBI-1532078), MSU, and the Murdock Charitable Trust Foundation (2015066:MNL). Funding for the mass spectrometry facility was provided in part by NIH NIGMS (P20GM103474 and S10OD28650), the Murdock Charitable Trust Foundation, and MSU. We are grateful to Brian Tripet for assistance with NMR studies and to Collin Stein for assistance with experiments.

REFERENCES

1. Rio, J.; Liang, H.; Perrin, M.-E. L.; Perego, L. A.; Grimaud, L.; Payard, P.-A. We Already Know Everything about Oxidative Addition to Pd(0): Do We? *ACS Catal.* **2023**, *13*, 11399–11421.

2. a) Hartwig, J. F. *Organotransition Metal Chemistry: From Bonding to Catalysis*. University Science Books, 2010; (b) Crabtree, R. H. *The Organometallic Chemistry of the Transition Metals, 6th ed.* John Wiley & Sons, 2014; (c) Labinger, J. A. Tutorial on Oxidative Addition. *Organometallics,* **2015**, *34*, 4784–4795.

3. Besora, M.; Maseras, F. The diverse mechanisms for the oxidative addition of C–Br bonds to $Pd(PR_3)$ and $Pd(PR_3)_2$ complexes. *Dalton Trans.* **2019**, *48*, 16242–16248.

4. Maes, B. U. W.; Verbeeck, S.; Verhelst, T.; Ekomié, A.; von Wolff, N.; Lefèvre, G.; Mitchell, E. A.; Jutand, A. Oxidative Addition of Haloheteroarenes to Palladium(0): Concerted versus S_NAr-Type Mechanism. *Chem. Eur. J.* **2015**, *21*, 7858–7865.

5. While all of these terms are useful, we tend to prefer "nucleophilic displacement" to avoid confusion about site-selectivity. In particular, a true metal-free S_NAr mechanism favors reaction at the C4-site of 2,4-dichloropyridine, whereas the "S_NAr-like" (nucleophilic displacement) mechanism for oxidative addition of this same substrate leads to selectivity for the C2 position (*vide infra* and ref 6a).

6. (a) Norman, J. P.; Larson, N. G.; Neufeldt, S. R. Different Oxidative Addition Mechanisms for 12- and 14-Electron Palladium(0) Explain Ligand-Controlled Divergent Site Selectivity. *ACS Catalysis* **2022**, *12*, 8822–8828; (b) Norman, J. P.; Larson, N. G.; Entz, E. D.; Neufeldt, S. R. Unconventional Site-Selectivity in Palladium-Catalyzed Cross-Couplings of Dichloroheteroarenes under Ligand-Controlled and Ligand-Free Systems. *J. Org. Chem.* **2022**, *87*, 7414–7421.

7. Senn, H. M.; Ziegler, T. Oxidative Addition of Aryl Halides to Palladium(0) Complexes: A Density-Functional Study Including Solvation. *Organometallics* **2004**, *23*, 2980–2988.

8. Joy, J.; Stuyver, T.; Shaik, S. Oriented External Electric Fields and Ionic Additives Elicit Catalysis and Mechanistic Crossover in Oxidative Addition Reactions. *J. Am. Chem. Soc.* **2020**, *142*, *8*, 3836–3850.

9. Gómez-Orellan, P.; Lledós, A.; Ujaque, G. Computational Analysis on the Pd-Catalyzed C–N Coupling of Ammonia with Aryl Bromides Using a Chelate Phosphine Ligand. *J. Org. Chem.* **2021**, *86*, 4007–4017.

10. Lyngvi, E.; Schoenebeck, F. Oxidative addition transition states of Pd(0) complexes in polar solvent—a DFT study involving implicit and explicit solvation. *Tetrahedron* **2013**, *69*, 5715–5718.

11. Lu, J.; Donnecke, S.; Paci, I.; Leitch, D. C. A reactivity model for oxidative addition to palladium enables quantitative predictions for catalytic cross-coupling reactions. *Chem. Sci.* **2022**, *13*, 3477–3488.

12. Fauvarque, J.-F.; Pflüger, F. Kinetics of oxidative addition of zerovalent palladium to aromatic iodides. *J. Organomet. Chem.* **1981**, *208*, 419-427.

13. Amatore, C.; Pflüger, F. Mechanism of oxidative addition of palladium(0) with aromatic iodides in toluene, monitored at ultramicroelectrodes. *Organometallics* **1990**, *9*, 2276–2282.

14. Portnoy, M.; Milstein, D. Mechanism of Aryl Chloride Oxidative Addition to Chelated Palladium(0) Complexes *Organometallics* **1993**, *12*, 1665–1673.

15. For other discussions of the role of solvent on mechanism, see refs 7, 8, and 10.

16. Lu, J.; Schley, N. D.; Paci, I.; Leitch, D. C. Mechanisms and Site Selectivity of (Het)Ar–X Oxidative Addition to Pd(0) Are Controlled by Frontier Molecular Orbital Symmetry. *ChemRxiv* **2024**; preprint. DOI: 10.26434/chemrxiv-2024-lrdz4 (accessed 2024-04-01).

17. Gaussian 16, Revision C.01, Frisch, M. J.; Trucks, G. W.; Schlegel, H. B.; Scuseria, G. E.; Robb, M. A.; Cheeseman, J. R.; Scalmani, G.; Barone, V.; Petersson, G. A.; Nakatsuji, H.; Li, X.; Caricato, M.; Marenich, A. V.; Bloino, J.; Janesko, B. G.; Gomperts, R.; Mennucci, B.; Hratchian, H. P.; Ortiz, J. V.; Izmaylov, A. F.; Sonnenberg, J. L.; Williams-Young, D.; Ding, F.; Lipparini, F.; Egidi, F.; Goings, J.; Peng, B.; Petrone, A.; Henderson, T.; Ranasinghe, D.; Zakrzewski, V. G.; Gao, J.; Rega, N.; Zheng, G.; Liang, W.; Hada, M.; Ehara, M.; Toyota, K.; Fukuda, R.; Hasegawa, J.; Ishida, M.; Nakajima, T.; Honda, Y.; Kitao, O.; Nakai, H.; Vreven, T.; Throssell, K.; Montgomery, J. A., Jr.; Peralta, J. E.; Ogliaro, F.; Bearpark, M. J.; Heyd, J. J.; Brothers, E. N.; Kudin, K. N.; Staroverov, V. N.; Keith, T. A.; Kobayashi, R.; Normand, J.; Raghavachari, K.; Rendell, A. P.; Burant, J. C.; Iyengar, S. S.; Tomasi, J.; Cossi, M.; Millam, J. M.; Klene, M.; Adamo, C.; Cammi, R.; Ochterski, J. W.; Martin, R. L.; Morokuma, K.; Farkas, O.; Foresman, J. B.; Fox, D. J. Gaussian, Inc., Wallingford CT, 2016.

18. Cossi, M.; Rega, N.; Scalmani, G.; Barone, V. Energies, structures, and electronic properties of molecules in solution with the C-PCM solvation model. *J. Comput. Chem.* **2003**, *24*, 669-681.

19. Yu, H. S.; He, X.; Truhlar, D. G. : A New Local Exchange-Correlation Functional for Kohn–Sham Density Functional Theory with Broad Accuracy for Atoms, Molecules, and Solids. *J. Chem. Theory Comput.* **2016**, *12*, 1280.

20. Hay, P. J.; Wadt, W. R. Ab initio effective core potentials for molecular calculations. Potentials for K to Au including the outermost core orbitals. *J. Chem. Phys.* **1985**, *82*, 299-310.

21. The MN15L functional was selected in part on the basis of (a) prior studies on related systems for which this method gave results consistent with experiment (see ref 22); and (b) its accuracy in benchmarking studies with some transition metal complexes: Moltved, K. A.; Kepp, K. P.; Chemical Bond Energies of 3d Transition Metals Studied by Density Functional Theory. *J. Chem. Theory Comput.* **2018**, *14*, 3479–3492.

22. Elias, E. K.; Rehbein, S. M.; Neufeldt, S. R. Solvent coordination to palladium can invert the selectivity of oxidative addition *Chem. Sci.* **2022**, *13*, 1618–1628.

23. Ribeiro, R.F.; Marenich, A.V.; Cramer, C.J.; Truhlar, D.G. Use of Solution-Phase Vibrational Frequencies in Continuum Models for the Free Energy of Solvation. *J. Phys. Chem. B.* **2011**, *115*, 14556.

24. The four ligands considered for describing palladium's geometry are the two phosphines and the two atoms of the breaking C—X bond. The observed geometry trends for these mechanisms are consistent with Senn and Ziegler's observations (ref 7).

25. The four ligands considered for describing palladium's geometry are the two phosphines, the *ipso* carbon, and the *ortho* atom with which Pd interacts.

26. Firsan, S.; Sivakumar, V.; Colacot, T. J. Emerging Trends in Cross-Coupling: Twelve-Electron-Based L1Pd(0) Catalysts, Their Mechanism of Action, and Selected Applications. *Chem. Rev.* **2022**, *122*, 16983–17027.

27. The natural bite angles of dppm, dppe, and Xantphos have been reported as 73°, 86°, and 108°, respectively; see: Birkholz, M.-N.; Freixa, Z.; van Leeuwen, P. W. N. M. Bite angle effects of diphosphines in C—C and C—X bond forming cross coupling reactions. *Chem. Soc. Rev.* **2009**, *38*, 1099–1118.

28. The calculated bite angles of dppm, dppe, dpppbz, and dcype in the π-complex between Pd(ligand) and PhCl are 71.6°, 88.3°, 84.1°, and 88.2°, respectively.

29. Yoshikai, N.; Matsuda, H.; Nakamura, E. Ligand Exchange as the First Irreversible Step in the Nickel-Catalyzed Cross-Coupling Reaction of Grignard Reagents. *J. Am. Chem. Soc.* **2008**, *130*, 15258–15259.

30. The calculated bite angle of Xantphos in the π-complex between Pd(Xantphos) and PhCl is 109.8°.

31. Single point energy calculations on several optimized geometries using different functionals led to predicted trends that were largely consistent across methods, although there are some exceptions (see page S35).

32. Although the immediate products of a displacement-type oxidative addition are cationic Pd(II) and (pseudo)halide, these can quickly collapse to form a neutral Pd(II)(X) product that is identical to the product formed by a concerted mechanism: see ref 7 for discussion.

33. Singleton, D. A.; Thomas, A. A. High-Precision Simultaneous Determination of Multiple Small Kinetic Isotope Effects at Natural Abundance. J. Am. Chem. Soc. 1995, 117, 9357–9358.

34. Dale, H. J. A.; Leach, A. G.; Lloyd-Jones, G. C. Heavy-Atom Kinetic Isotope Effects: Primary Interest or Zero Point? *J. Am. Chem. Soc.* **2021**, *143*, 21079–21099.

35. Paton, R. S. *Kinisot.py*, version 2.0.2; Zenodo, 2023; DOI: 10.5281/zenodo.10403662.

36. The relative energetics of π-complexation and C—X cleavage can be highly sensitive to DFT method, in particular with bulky monodentate ligands: (a) McMullin, C. L.; Jover, J.; Harvey, J. N.; Fey, N. Accurate modelling of Pd(0) + PhX oxidative addition kinetics. *Dalton Trans.* **2010**, *39*, 10833–10836; (b) McMullin, C. L.; Fey, N.; Harvey, J. N. Computed ligand effects on the oxidative addition of phenyl halides to phosphine supported palladium(0) catalysts. *Dalton Trans.* **2014**, *43*, 13545–13556; (c) Larson, N. G.; Norman, J. P.; Neufeldt, S. R. Mechanistic Origin of Ligand Effects on Exhaustive Functionalization During Pd-Catalyzed Cross-Coupling of Dihaloarenes. *ACS Catal.* **2024**, *14*, 7127–7135.

37. (a) Schoenebeck, F.; Houk, K. N. Ligand-Controlled Regioselectivity in Palladium-Catalyzed Cross Coupling Reactions *J. Am. Chem. Soc.* **2010**, *132*, 2496–2497; (b) Lyngvi, E.; Sanhueza, I. A.; Schoenebeck, F. Dispersion Makes the Difference: Bisligated Transition States Found for the Oxidative Addition of $Pd(PtBu_3)_2$ to Ar-OSO_2R and Dispersion-Controlled Chemoselectivity in Reactions with $Pd[P(iPr)(tBu_2)]_2$. *Organometallics* **2015**, *34*, 805–812. (c) Niemeyer, Z. L.; Milo, A.; Hickey, D. P.; Sigman, M. S. Parameterization of phosphine ligands reveals mechanistic pathways and predicts reaction outcomes. *Nature Chem.* **2016**, *8*, 610–617.

38. Newman-Stonebraker, S. H.; Smith, S. R.; Borowski, J. E.; Peters, E.; Gensch, T.; Johnson, H. C.; Sigman, M. S.; Doyle, A. G. Univariate classification of phosphine ligation state and reactivity in cross-coupling catalysis. *Science*, **2021**, *374*, 301–308.

39. (a) Melander, L. C. & Saunders, W. H. Reaction Rates of Isotopic Molecules (Wiley, New York, NY, 1980); (b) Kwan, E. E.; Zeng, Y.; Besser, H. A.; Jacobsen, E. N. Concerted nucleophilic aromatic substitutions. *Nature Chem.* **2018**, *10*, 917–923.

40. Joshi, C.; Macharia, J. M.; Izzo, J. A.; Wambua, V.; Kim, S.; Hirschi, J. S.; Vetticatt, M. J. Isotope Effects Reveal the Catalytic Mechanism of the Archetypical Suzuki-Miyaura Reaction. *ACS Catal.* **2022**, *12*, 2959–2966.

41. Galardon, E.; Ramdeehul, S.; Brown, J. M.; Cowley, A.; Hii, K. K.; Jutand, A. Profound Steric Control of Reactivity in Aryl Halide Addition to Bisphosphane Palladium(0) Complexes. *Angew. Chem. Int. Ed.* **2002**, *41*, 1760–1763.

42. For other reports examining the role of molecular orbital symmetry during oxidative addition (or reductive elimination) at Pd^0, see refs 47b, 47c and (a) Tatsumi, K.; Hoffmann, R.; Yamamoto, A.; Stille, J. K. Reductive Elimination of d^8-Organotransition Metal Complexes. *Bull. Chem. Soc. Jpn.* **1981**, *54*, 1857–1867; (b) Ariafard, A.; Yates, B. F. In-depth insight into the electronic and steric effects of phosphine ligands on the mechanism of the R–R reductive elimination from $(PR_3)_2PdR_2$. *J. Organomet Chem.* **2009**, *694*, 2075-2084; (c) Wolters, L. P.; van Zeist, W.-J.; Bickelhaupt, F. M. New Concepts for Designing d^{10}-$M(L)_n$ Catalysts: d Regime, s Regime and Intrinsic Bite-Angle Flexibility. *Chem. Eur. J.* **2014**, *20*, 11370–11381; (d) Wolters, L. P.; Bickelhaupt, F. M. Selective C–H and C–C Bond Activation: Electronic Regimes as a Tool for Designing d^{10} ML_n Catalysts. *Chem. Asian. J.* **2015**, *10*, 2272–2282.

43. In prior computational studies on concerted reductive eliminations (refs 42a and 42b), Pd has been shown to react faster when it is effectively 3-coordinate in the transition state (reaction at PdL) rather than 4-coordinate (reaction at PdL_2) due to orbital considerations. Along the same lines, it is noteworthy that a displacement mechanism for oxidative addition at PdL_2 leads to a 3-coordinate complex as the immediate product, whereas a concerted mechanism at PdL_2 results in a 4-coordinate complex.

44. Bickelhaupt, F. M.; Houk, K. N. Analyzing Reaction Rates with the Distortion/Interaction-Activation Strain Model. *Angew. Chem., Int. Ed.* **2017**, *56*, 10070–10086.

45. We note, however, that reaction of PhCl at $Pd(PCy_3)_2$ is likely not experimentally relevant, since kinetic studies indicate that the first irreversible step of this reaction occurs at monoligated $Pd(PCy_3)$ (see ref 46). Interestingly, DFT calculations are unable to reproduce this conclusion (see ref 36b). For a similar distortion-interaction analysis using PhBr (for which reaction at $Pd(PCy_3)_2$ may occur), see pages S36-S37.

46. Barrios-Landeros, F.; Carrow, B. P.; Hartwig, J. F. Effect of Ligand Steric Properties and Halide Identity on the Mechanism for Oxidative Addition of Haloarenes to Trialkylphosphine Pd(0) Complexes, *J. Am. Chem. Soc.* ***2009***, *131*, 8141–8154.

47. (a) Kranenburg, M., Kamer, P. C. J.; van Leeuwen, P. W. N. M. The Effect of the Bite Angle of Diphosphane Ligands on Activity and Selectivity in Palladium-Catalyzed Allylic Alkylation. *Eur. J. Inorg. Chem.* **1998**, 25–27; (b) van Zeist, W.-J.; Visser, R.; Bickelhaupt, F. M. The Steric Nature of the Bite Angle. *Chem. Eur. J.* **2008**, *15*, 6112–6115; (c) van Zeist, W.-J.; Bickelhaupt, F. M. Steric nature of the bite angle. A closer and a broader look. *Dalton Trans.* **2011**, *40*, 3028–3038.

48. Jutand, A.; Mosleh, A. Rate and Mechanism of Oxidative Addition of Aryl Triflates to Zerovalent Palladium Complexes. Evidence for the Formation of Cationic σ-Aryl Pd Complexes. *Organometallics* **1995**, *14*, 1810–1817.

49. Roy, A. H.; Hartwig, J. F. Oxidative Addition of Aryl Sulfonates to Palladium(0) Complexes of Mono- and Bidentate Phosphines. Mild Addition of Aryl Tosylates and the Effects of Anions on Rate and Mechanism. *Organometallics* **2004**, *23*, 194–202.

50. (a) Louie, J.; Driver, M. S.; Hamann, B. C.; Hartwig, J. F. Palladium-Catalyzed Amination of Aryl Triflates and Importance of Triflate Addition Rate. *J. Org. Chem.* **1997**, *62*, 1268–1273; (b) Littke, A. F.; Dai, C.; Fu, G. C. Versatile Catalysts for the Suzuki Cross-Coupling of Arylboronic Acids with Aryl and Vinyl Halides and Triflates under Mild Conditions. *J. Am. Chem. Soc.* **2000**, *122*, 4020–4028; (c) Reeves, E. K.; Humke, J. N.; Neufeldt, S. R.

N-Heterocyclic Carbene Ligand-Controlled Chemodivergent Suzuki–Miyaura Cross Coupling. *J. Org. Chem.* **2019**, *84*, 11799–11812.

51. Paenurk, E.; Kaupmees, K.; Himmel, D.; Kütt, A.; Kaljurand, I.; Koppel, I. A.; Krossing, I.; Leito, I. A unified view to Brønsted acidity scales: do we need solvated protons? *Chem. Sci.* **2017**, *8*, 6964–6973.

52. (a) Fairlamb, I. J. S. Regioselective (site-selective) functionalisation of unsaturated halogenated nitrogen, oxygen and sulfur heterocycles by Pd-catalysed cross-couplings and direct arylation processes. *Chem. Soc. Rev.* **2007**, *36*, 1036–1045; (b) Almond-Thynne, J.; Blakemore, D. C.; Pryde, D. C.; Spivey, A. C. Site-selective Suzuki– Miyaura coupling of heteroaryl halides – understanding the trends for pharmaceutically important classes. *Chem. Sci.* **2017**, *8*, 40–62. (c) Palani, V.; Perea, M. A.; Sarpong, R. Site-Selective Cross- Coupling of Polyhalogenated Arenes and Heteroarenes with Identical Halogen Groups. *Chem. Rev.* **2022**, *122*, 10126–10169; (d) Norman, J. P.; Neufeldt, S. R. The Road Less Traveled: Unconventional Site Selectivity in Palladium-Catalyzed Cross-Couplings of Dihalogenated N-Heteroarenes. *ACS Catal.* **2022**, *12*, 12014–12026.

53. (a) Legault, C. Y.; Garcia, Y.; Merlic, C. A.; Houk, K. N. Origin of Regioselectivity in Palladium-Catalyzed Cross-Coupling Reactions of Polyhalogenated Heterocycles. *J. Am. Chem. Soc.* **2007**, *129*, 12664–12665; (b) Garcia, Y.; Schoenebeck, F.; Legault, C. Y.; Merlic, C. A.; Houk, K. N. Theoretical Bond Dissociation Energies of Halo- Heterocycles: Trends and Relationships to Regioselectivity in Palladium-Catalyzed Cross-Coupling Reactions. *J. Am. Chem. Soc.* **2009**, *131*, 6632–6639.

54. Yang, M.; Chen, J.; He, C.; Hu, X.; Ding, Y.; Kuang, Y.; Liu, J.; Huang, Q. Palladium-Catalyzed C-4 Selective Coupling of 2,4- Dichloropyridines and Synthesis of Pyridine-Based Dyes for Live-Cell Imaging. *J. Org. Chem.* **2020**, *85*, 6498–6508.

55. Scott, N. W. J.; Ford, M. J.; Jeddi, N.; Eyles, A.; Simon, L.; Whitwood, A. C.; Tanner, T.; Willans, C. E.; Fairlamb, I. J. S. A Dichotomy in Cross-Coupling Site Selectivity in a Dihalogenated Heteroarene: Influence of Mononuclear Pd, Pd Clusters, and Pd Nanoparticles–the Case for Exploiting Pd Catalyst Speciation. *J. Am. Chem. Soc.* **2021**, *143*, 9682–9693.

56. (a) Kikuchi, O.; Hondo, Y.; Morihashi, K.; Nakayama, M. An Ab Initio Molecular Orbital Study of Pyridyl Radicals. *Bull. Chem. Soc. Jpn.* **1988, *61***, 291–292; (b) Jones, J.; Bacskay, G. B.; Mackie, J. C.; Doughty, A. Ab Initio Studies of the Thermal Decomposition of Azaaromatics: Free Radical versus Intramolecular Mechanism. *J. Chem. Soc. Faraday Trans.* **1995**, *91*, 1587–1592.

57. Bingham, R. C. Lone Pair-Polar Bond Hyperconjugation in Carbon-Halogen Chemistry. *J. Am. Chem. Soc.* **1975**, *97*, 6743–6746.

58. The Pd---N distance in the displacement mechanism for 2-chloropyridine with $Pd(PCy_3)_2$ is 2.19 Å, which is very similar to the Pd---N distance of a fully formed bond in $(PMe_3)Pd^{II}(Ph)(Cl)$(pyridine) (2.18 Å).

59. Bite angles of dppf and dtbpf have been reported to be 99° (see ref 27) and 104.2°: Grasa, G. A.; Colacot, T. J. α-Arylation of Ketones Using Highly Active, Air-Stable $(DtBPF)PdX_2$ (X = Cl, Br) Catalysts. *Org. Lett.* **2007**, *9*, 5489–5492.

60. For results using the other bisphosphines from Figure 2, please see Tables S12-S14.

61. Ji, J.; Li, T.; Bunnelle, W. H. Selective Amination of Polyhalopyridines Catalyzed by a Palladium–Xantphos Complex. *Org. Lett.* **2003**, *5*, 4611–4614.

62. Keylor, M. H.; Niemeyer, Z. L.; Sigman, M. S.; Tan, K. L. Inverting Conventional Chemoselectivity in Pd-Catalyzed Amine Arylations with Multiply Halogenated Pyridines. *J. Am. Chem. Soc.* **2017**, *139*, 10613–10616.

63. Notably, factors like solvent polarity or additional substituents on the aryl electrophile, factors that were not considered in this work, may complicate predictions (see ref 16). Additionally, unsymmetrical ligands (such as Buchwald-type biaryl phosphines) were not evaluated in these studies due to their computational complexity, although further investigation is ongoing. Lastly, when extrapolating predicted mechanism to the concept of site-selectivity, it is worth noting that catalyst speciation as PdL versus PdL_2 is not always straightforward (for example, see ref 45 and refs 4, 38, and 40) and that formation of multinuclear Pd species may lead to unexpected selectivity (see refs 6b and 55).